Anal. Chem. **2007,** *79,* 8391−8398

Electrochemical Impedance Spectroscopy for Investigations on Ion Permeation in ω-Functionalized Self-Assembled Monolayers

Fredrik Björefors,* Rodrigo M. Petoral, Jr., and Kajsa Uvdal

Division of Sensor Science and Molecular Physics, Department of Physics, Chemistry and Biology (IFM), Linköping University, SE-581 83 Linköping, Sweden

Electrochemical impedance spectroscopy was employed to explore the possibility of relating the permeation of electrolyte ions in ω-functionalized self-assembled monolayers to structural or polarity changes induced by interaction with metal ions. The monolayers were based on alkanethiols modified with a phosphorylated tyrosine analogue, which from previous work are known to drastically change their organization on gold surfaces upon interaction with aluminum and magnesium ions. The ion permeation was evaluated by using relatively low excitation frequencies, 1000 to 2 Hz, and quantified by an extra resistive component in the equivalent circuit (R_{SAM}). The extent of ion permeation influenced by the dc potential, the electrolyte concentration, the functional group, and the thiol length were also investigated. It was, for example, found that R_{SAM} decreased ~20% when the thiol organization collapsed and that R_{SAM} increased ~4−5 times when the electrolyte concentration was decreased by 1 order of magnitude. Interesting observations were also made regarding the potential dependence of R_{SAM} and the double layer capacitance. The evaluation of the ion permeation can be used to indirectly detect whether the organization of a SAM is influenced by, for example, electric fields or chemical and biological interactions. This analysis can be performed without addition of redox species, but is on the other hand complicated by the fact that other factors also influence the presence of ions within the monolayer. In addition, a second parallel *RC* process was obtained in some of the impedance spectra when using even lower frequencies, and its resistive component revealed different results compared to R_{SAM}. Such data may be useful for the understanding of complex double layer phenomena at modified electrodes.

Electrochemical techniques offer some unique advantages for the evaluation of thiol-based self-assembled monolayers (SAMs) immobilized on metal substrates. Cyclic voltammetry (CV) can be employed to obtain qualitative information on the thiol organization and insulating properties via both faradaic and nonfaradaic currents, while oxidation or reduction of the thiols on the surface can reveal both the binding strength and the number of thiols immobilized on the electrode.[1−4] CV and electrochemical impedance spectroscopy (EIS) have also been employed for more fundamental studies, involving, for example, charge transfer via redox groups within the SAM itself,[1,2,5−9] and investigations on interfacial properties and double layer phenomena.[1,2,10−16] SAMs modified with acid−base groups have, for instance, been important for connecting double layer models with electrochemical theory and experiments.[11−16] Both CV and EIS are frequently employed for direct or indirect detection of chemical and biological reactions and interactions at ω-functionalized SAMs, with the aim of developing sensors and detectors.[3,17−25]

* To whom correspondence should be addressed. E-mail: frebj@ifm.liu.se, Fax: +46 13 288969.

(1) Bard, A. J.; Abruna, H. D.; Chidsey, C. E.; Faulkner, L. R.; Feldberg, S. W.; Itaya, K.; Majda, M.; Melroy, O.; Murray, R. W.; Porter, M. D.; Soriaga, M. P.; White, H. S. *J. Phys. Chem.* **1993**, *97*, 7147−7173.
(2) Finklea, H. O. Electrochemistry of Organized Monolayers of Thiols and Related Molecules on Electrodes, In *Electroanalytical Chemistry*; Bard, A. J., Rubinstein, I., Eds.; Marcel Dekker: New York, 1996; Vol. 19, pp 109−335.
(3) Flink, S.; van Veggel, F.; Reinhoudt, D. N. *Adv. Mater.* **2000**, *12*, 1315−1328.
(4) Chen, D.; Wang, G.; Li, J. H. *J. Phys. Chem. C* **2007**, *111*, 2351−2367.
(5) Smalley, J. F.; Finklea, H. O.; Chidsey, C. E. D.; Linford, M. R.; Creager, S. E.; Ferraris, J. P.; Chalfant, K.; Zawodzinsk, T.; Feldberg, S. W.; Newton, M. D. *J. Am. Chem. Soc.* **2003**, *125*, 2004−2013.
(6) Sek, S.; Misicka, A.; Bilewicz, R. *J. Phys. Chem. B* **2000**, *104*, 5399−5402.
(7) Andreu, R.; Calvente, J. J.; Fawcett, W. R.; Molero, M. *J. Phys. Chem. B* **1997**, *101*, 2884−2894.
(8) Walter, D. G.; Campbell, D. J.; Mirkin, C. A. *J. Phys. Chem. B* **1999**, *103*, 402−405.
(9) Calvente, J. J.; Lopez-Perez, G.; Ramirez, P.; Fernandez, H.; Zon, M. A.; Mulder, W. H.; Andreu, R. *J. Am. Chem. Soc.* **2005**, *127*, 6476−6486.
(10) Becka, A. M.; Miller, C. J. *J. Phys. Chem.* **1993**, *97*, 6233−6239.
(11) Smith, C. P.; White, H. S. *Langmuir* **1993**, *9*, 1−3.
(12) Fawcett, W. R.; Fedurco, M.; Kovacova, Z. *Langmuir* **1994**, *10*, 2403−2408.
(13) Bryant, M. A.; Crooks, R. M. *Langmuir* **1993**, *9*, 385−387.
(14) Kakiuchi, T.; Iida, M.; Imabayashi, S.; Niki, K. *Langmuir* **2000**, *16*, 5397−5401.
(15) Schweiss, R.; Werner, C.; Knoll, W. *J. Electroanal. Chem.* **2003**, *540*, 145−151.
(16) Burshtain, D.; Mandler, D. *Chemphyschem* **2004**, *5*, 1532−1539.
(17) Gooding, J. J.; Mearns, F.; Yang, W. R.; Liu, J. Q. *Electroanalysis* **2003**, *15*, 81−96.
(18) Wink, T.; vanZuilen, S. J.; Bult, A.; vanBennekom, W. P. *Analyst* **1997**, *122*, R43−R50.
(19) Terrettaz, S.; Vogel, H.; Grätzel, M. *J. Electroanal. Chem.* **1992**, *326*, 161−176.
(20) Flink, S.; Boukamp, B. A.; van den Berg, A.; van Veggel, F.; Reinhoudt, D. N. *J. Am. Chem. Soc.* **1998**, *120*, 4652−4657.
(21) Stora, T.; Hovius, R.; Dienes, Z.; Pachoud, M.; Vogel, H. *Langmuir* **1997**, *13*, 5211−5214.
(22) Turyan, I.; Mandler, D. *Anal. Chem.* **1997**, *69*, 894−897.
(23) Bart, M.; Stigter, E. C. A.; Stapert, H. R.; de Jong, G. J.; van Bennekom, W. P. *Biosens. Bioelectron.* **2005**, *21*, 49−59.

10.1021/ac071399d CCC: $37.00
Published on Web 09/29/2007

Although a substantial number of papers on these topics exist, relatively few studies have focused on EIS and nonfaradaic currents for the evaluation of the permeation of ions within SAMs. Fawcett et al.[26−29] and Boubour and Lennox[30,31] have in a number of papers explored the use of EIS and relatively low excitation frequencies to also include time constants relevant for ions and solvent molecules inside various SAMs. For monolayers based on ω-hydroxydecanethiol and 4′-hydroxy-4-mercaptobiphenyl, Fawcett et al.[26] found a parallel conduction pathway having a relaxation time on the order of seconds to minutes. The authors concluded that this could be related either to ion permeation into the bulk of the SAM or to reorientation of the thiols on the electrode surface. Boubour and Lennox[30,31] also performed similar experiments to demonstrate the importance of ion and solvent permeation into potential-induced defects in SAMs. When using several ω-functionalized thiols with different lengths, they could via ion permeation identify critical potentials where the electric and electrochemical properties of the SAMs were significantly altered. In these studies,[26−31] the ion permeation resulted in a semicircle in the impedance spectra and was hence evaluated by using an equivalent circuit including a resistance in parallel to the double layer capacitance. To further understand the ion permeation inside SAMs, Fawcett et al. also conducted EIS experiments in the presence of redox species[27,28] and by using different temperatures and propylene carbonate as solvent.[29] Some of the papers above also reported the presence of a second parallel *RC* process in the impedance spectra.[26,30,31] Although the exact physical and chemical interpretation of the extra R and C components representing this process were not fully known, they may help to reveal more information on SAM structures and double layer phenomena. The resistive properties of SAMs have also been evaluated when used as templates for biomolecular interactions[23,32] and lipid membranes,[33] as well as for corrosion inhibition[34] and thiol-protected gold nanoparticles.[35] In a more general perspective, nonfaradaic currents with respect to the presence of ions in other types of surface modifications have naturally also been studied in detail. Examples include polyelectrolytes, bilayer membranes, conducting polymers, and corrosion protective coatings.

The aim of this paper was to use EIS and relatively low excitation frequencies to investigate the possibility to obtain information on ω-functionalized SAMs via ion permeation, especially related to changes in the SAM structure induced by a chemical interaction. On the basis of previous work, we have demonstrated that metal ions could coordinate to SAMs modified with phosphorylated amino acid analogues[24,25] and that phosphorylated tyrosine SAMs significantly change their organization when aluminum or magnesium ions are coordinated to the phosphate groups.[25] The latter observation was made by CV and infrared- and X-ray photoelectron spectroscopy, and the structural collapse is likely to increase the number of ions and solvent molecules within the SAM. The present aim was also to try to understand the influence from the SAM thickness, the functional group, the supporting electrolyte concentration, and the electrode dc potential on the extent of ion permeation. The consideration of ion permeation is important when SAMs are employed as model systems for fundamental interfacial and charge-transfer studies and when used as templates for sensors and detectors. An additional aim was also to demonstrate interesting double layer phenomena experienced when using even lower excitation frequencies (down to 0.1 Hz).

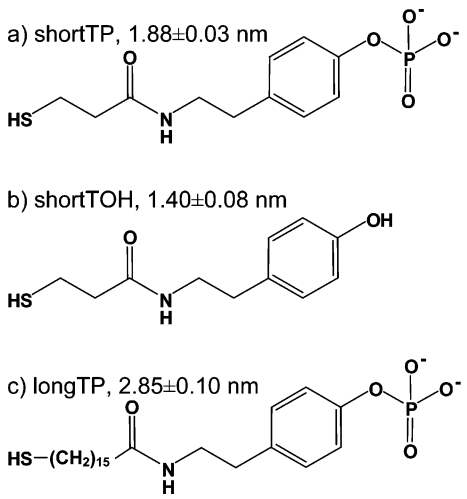

Figure 1. Abbreviations and schematic illustrations of the tyrosine analogue thiols used in this study. The numbers after the abbreviations refer to the ellipsometric thickness of the resulting SAMs.[25,36] (a) Phosphorylated tyrosine-terminated propanethiol (shortTP), (b) the corresponding nonphosphorylated thiol (shortTOH), and (c) phosphorylated tyrosine thiol with 15 methylene units (longTP).

EXPERIMENTAL SECTION

Assembly. The substrates used for assembly were 15 × 20 mm gold-coated (200 nm) glass plates. Prior to assembly, the gold substrates were cleaned in TL1, a 5:1:1 mixture of MQ water (Millipore), 30% hydrogen peroxide (Merck), and 25% ammonia (Merck), at 80 °C for 5 min. The tyrosine analogue thiols used to form the monolayers are displayed in Figure 1. The thiol in Figure 1a, a phosphorylated tyrosine-terminated propanethiol (shortTP), was used to coordinate aluminum ions. For comparison, the corresponding nonphosphorylated thiol (shortTOH) in Figure 1b was used. Monolayers based on phosphorylated tyrosine thiols with 15 methylene units (longTP, Figure 1c) were also assembled in order to investigate the influence from the thiol length. The phosphorylated tyrosine SAMs were prepared by placing the gold surfaces in ethanol solutions (Kemetyl, Haninge, Sweden) with a thiol concentration of 1 mM for at least 16 h. For solubility reasons, the phosphate group in the thiol with the longest methylene chain contained two protective *tert*-butyl groups.[36] After assembly, they

(24) Ekeroth, J.; Konradsson, P.; Björefors, F.; Lundström, I.; Liedberg, B. *Anal. Chem.* **2002**, *74*, 1979−1985.
(25) Petoral, R. M.; Björefors, F.; Uvdal, K. *J. Phys. Chem. B* **2006**, *110*, 23410−23416.
(26) Janek, R. P.; Fawcett, W. R.; Ulman, A. *J. Phys. Chem. B* **1997**, *101*, 8550.
(27) Janek, R. P.; Fawcett, W. R.; Ulman, A. *Langmuir* **1998**, *14*, 3011−3018.
(28) Protsailo, L. V.; Fawcett, W. R. *Electrochim. Acta* **2000**, *45*, 3497−3505.
(29) Protsailo, L. V.; Fawcett, W. R. *Langmuir* **2002**, *18*, 8933−8941.
(30) Boubour, E.; Lennox, R. B. *J. Phys. Chem. B* **2000**, *104*, 9004−9010.
(31) Boubour, E.; Lennox, R. B. *Langmuir* **2000**, *16*, 7464−7470.
(32) Lasseter, T. L.; Cai, W.; Hamers, R. J. *Analyst* **2004**, *129*, 3−8.
(33) Han, X. J.; Critchley, K.; Zhang, L. X.; Pradeep, S. N. D.; Bushby, R. J.; Evans, S. D. *Langmuir* **2007**, *23*, 1354−1358.
(34) Jennings, G. K.; Munro, J. C.; Yong, T. H.; Laibinis, P. E. *Langmuir* **1998**, *14*, 6130−6139.
(35) Laaksonen, T.; Pelliniemi, O.; Quinn, B. M. *J. Am. Chem. Soc.* **2006**, *128*, 14341−14346.
(36) Ekeroth, J.; Björefors, F.; Borgh, A.; Lundström, I.; Liedberg, B.; Konradsson, P. *Anal. Chem.* **2001**, *73*, 4463−4468.

were removed by immersing the substrate in a 4:1 mixture of methylene chloride (Fischer) and trifluoroacetic acid (Fluka) for 20 min. The nonphosphorylated SAMs were prepared in the same way, but the solvent was in this case water at pH 12 (using NaOH).[25] After the preparation step, the substrates were rinsed in either ethanol or water, respectively, followed by ultrasonication for 3 min and further rinsing. To remove coordinated contaminants, the phosphorylated tyrosine SAMs were immersed in a 1 mM EDTA (Merck) solution for 1 min (followed by rinsing, 1 min extra ultrasonication, and further rinsing). Prior to use in experiments, all surfaces were dried under a stream of nitrogen. The resulting ellipsometric thicknesses are also displayed in Figure 1, while a full description of the synthesis and surface characterization of the SAMs can be found elsewhere.[24,25,36−39]

EIS Experiments. The impedance data were obtained with an Autolab PGSTAT30 (EcoChemie, Utrecht, The Netherlands), equipped with a FRA2 frequency response analyzer module. An Ag/AgCl electrode was used as reference electrode, while a folded platinum wire acted as the counter electrode. The SAM-coated gold surfaces (working electrodes) were brought into contact with the solution via press fitting to an O-ring in the side of the Kel-F-based electrochemical cell. The exposed area of the electrode was 0.20 cm^2. The centers of the reference- and counter electrodes were positioned 20 and 29 mm from the center of the working electrode, respectively. It was essential to put the entire setup in a Faraday cage (connected to the potentiostat ground) in order to minimize influence from the ambient. The parts of the cables from the potentiostat not covered with a grounded shield were also put in the cage (via a 26-mm hole on the back side).

The impedance data were recorded in the frequency range 1000 Hz down to either 0.5 or 0.1 Hz, with an rms amplitude of 5 mV. To clearly separate different relaxation processes, as many as 50 logarithmically distributed frequencies per decade were used. Below 0.1 Hz, the signal-to-noise ratio was too low, and the measurements naturally also became very time-consuming. In order to see the influence from different potentials, the dc level was varied between 0.0 and 0.4 V (vs Ag/AgCl). These potential limits were chosen to minimize influence from faradaic currents (primarily reduction of dissolved oxygen and oxidation of the gold substrate). The Autolab software FRA 4.9.005 was used to fit the impedance data to an appropriate equivalent circuit. To account for nonideal behavior, all capacitances were evaluated as a constant phase element (CPE),[2,40] for which the exponential factor varied between 0.97 and 0.98. The estimated error of the fit in percent (provided by the FRA software) for each component in the equivalent circuits was used to express the uncertainty. In Figures 4, 6, 8, and 9; the error bars correspond to the average error of the fit obtained for each separate SAM between 0.0 and 0.4 V in each supporting electrolyte concentration (the error bars in Figure 5 and 7 were omitted as they were smaller than the size of the markers). Addition of aluminum ions to the electrolyte (either 10 or 100 mM KNO_3 (Merck)) to a final concentration of 100 μM was made from an appropriate volume of 30 mM $Al(NO_3)_3 \cdot 9H_2O$ (Kebo, Germany), followed by manual stirring. The aluminum ion solution also contained 100 mM KNO_3. At least three separate electrodes were tested for each SAM in each supporting electrolyte concentration.

RESULTS AND DISCUSSION

To investigate the extent of ion permeation in ω-functionalized SAMs under different experimental conditions, three different tyrosine-terminated monolayers were prepared. The first one was based on phosphorylated tyrosine-terminated propanethiols (shortTP, Figure 1a), which form a 1.88 ± 0.03-nm-thick monolayer on gold. This monolayer has the ability to coordinate a number of divalent and trivalent cations.[25] For comparison, SAMs based on the corresponding nonphosphorylated thiols (shortTOH, Figure 1b), and longer phosphorylated tyrosine thiols (longTP, Figure 1c) were also prepared. The organization of the shortTP SAM is from previous work known to collapse when aluminum ions are coordinated to the phosphate groups.[25] X-ray photoelectron spectroscopy, for example, revealed a more compact orientation of the monolayer, where the phosphate groups were situated closer to the chemisorbed sulfur atoms, while infrared spectroscopy indicated a reorientation of the thiols on the surface to accommodate the aluminum ions. CV further showed that the blocking properties of the SAM were substantially decreased. In that work, EIS was used to evaluate the double layer capacitance to detect and quantify the coordination of aluminum ions. The frequency range used was 2000−200 Hz, which resulted in almost vertical lines in the impedance spectra. Consequently, a series $R_{sol}C_{dl,CPE}$ circuit, where R_{sol} represents the solution resistance and $C_{dl,CPE}$ the total differential double layer capacitance, was sufficient to model the impedance data. The impedance spectra in the present experiments when using frequencies from 1000 to 0.1 Hz were, however, found to reveal a more complex behavior. For the shortTP in 100 mM KNO_3, the first part of a semicircle was present from 1000 Hz down to ∼10−5 Hz, followed by the onset of a second (much larger) semicircle down to 0.1 Hz, as shown in Figure 2a and b. The first semicircle was also present for the shortTOH and longTP SAMs in practically the same frequency range, but a well-defined second semicircle could not be found for these two monolayers. Two differences were experienced for all SAMs when the lower supporting electrolyte concentration (10 mM KNO_3) was used. The influence from stray capacitances was then found to be significant at frequencies above 100 Hz, and those frequencies were hence omitted in the data evaluation. It was also found that the frequency range for the first semicircle was extended to slightly lower frequencies.

A semicircle in an impedance spectrum can, in the simplest case, be modeled with a resistance in parallel to the total double layer capacitance (see Figure 3a). The extra parallel resistance will in this case be used to describe the resistive properties of the SAMs and will for the first semicircle be denoted as R_{SAM}. The estimated errors of the fit obtained for R_{SAM} was normally between 3 and 7% and below 0.2% for $C_{dl,CPE}$. The first part of this paper focuses on the evaluation of the first semicircle and R_{SAM} for the three different monolayers when using the equivalent circuit in Figure 3a. The last part includes evaluation of the second *RC* process obtained for the shortTP SAM in 100 mM KNO_3. In an effort to simultaneously evaluate both *RC* processes, the equivalent circuits in Figure 3b and c were then also used.

(37) Ekeroth, J.; Borgh, A.; Konradsson, P.; Liedberg, B. *J. Colloid Interface Sci.* **2002**, *254*, 322−330.

(38) Uvdal, K.; Ekeroth, J.; Konradsson, P.; Liedberg, B. *J. Colloid Interface Sci.* **2003**, *260*, 361−366.

(39) Borgh, A.; Ekeroth, J.; Petoral, R. A.; Uvdal, K.; Konradsson, P.; Liedberg, B. *J. Colloid Interface Sci.* **2006**, *295*, 41−49.

(40) Macdonald, J. L. *Impedance Spectroscopy*; Wiley: New York, 1987.

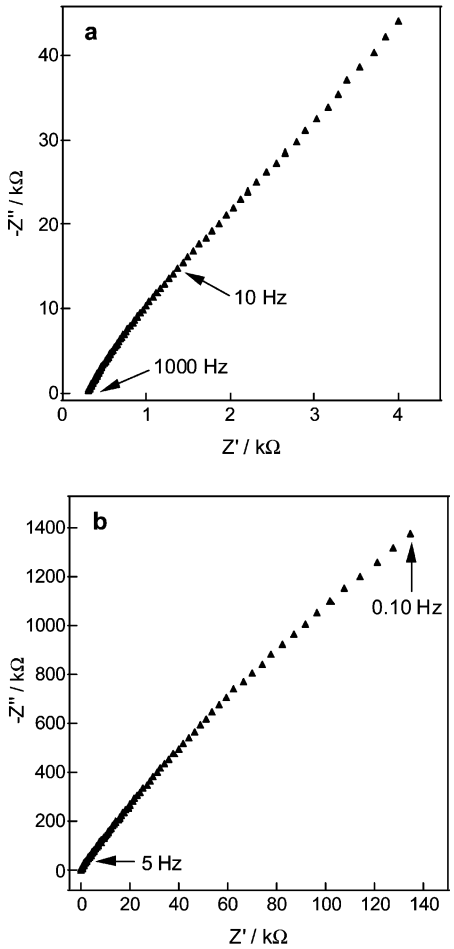

Figure 2. Impedance spectra showing the two *RC* processes obtained for the shortTP SAM in 100 mM KNO_3 at 0.0 V. The frequency ranges used for the following modeling were (a) 1000−10 and (b) 5−0.1 Hz, respectively.

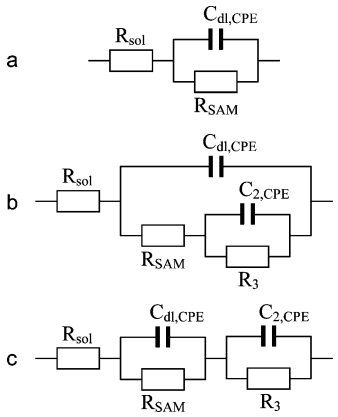

Figure 3. Equivalent circuits used for the evaluation of the impedance data. R_{sol} denotes the solution resistance, $C_{dl,CPE}$ the total differential double layer capacitance, and R_{SAM} was used to evaluate the ion permeation. $C_{2,CPE}$ and R_3 in (b) and (c) were used to model the second *RC* process described in the last part of the paper. To account for nonideal behavior, both capacitances were via the software evaluated as constant phase elements.

ShortTP SAM. Impedance spectra were recorded for the shortTP monolayer in 100 mM KNO_3 in the potential range 0.0−0.4 V (vs Ag/AgCl). The shortTP thiols are too short to form completely insulating SAMs; hence, electrolyte ions (and solvent molecules) were present in the monolayer from the beginning. As a consequence of the poorly insulating properties, the electrode potential had a major influence on R_{SAM}. From the top curve in Figure 4a, R_{SAM} reaches a maximum of almost 1.4 MΩ at ∼0.2 V and then decreases at more positive and negative potentials. However, when aluminum ions were added to the electrolyte, R_{SAM} decreased by 0.2−0.3 MΩ at potentials above 0.050 mV. The decreased resistance indicates that more ions were present in the SAM, and this was most likely due to the collapse in the thiol organization on the surface when aluminum ions were coordinated to the phosphate groups. The negative charges on the phosphates are also neutralized upon coordination, and this may also influence the extent of ion permeation, although difficult to quantify and separate from the structural change. However, to first verify that R_{SAM} was related to the number of electrolyte ions, the same experiments were performed in a solution where the electrolyte concentration was lowered by 1 order of magnitude, i.e., to 10 mM KNO_3. The solution resistance was in this case increased from 330 Ω to 2.3 kΩ and, as expected, it also had a significant influence on the values of R_{SAM}, which now were 4−5 times higher (Figure 4b). The influence from electrode potential and the addition of aluminum ions were on the other hand basically the same. Interestingly, R_{SAM} increased ∼4−5 times, when the supporting electrolyte concentration was decreased 10 times,

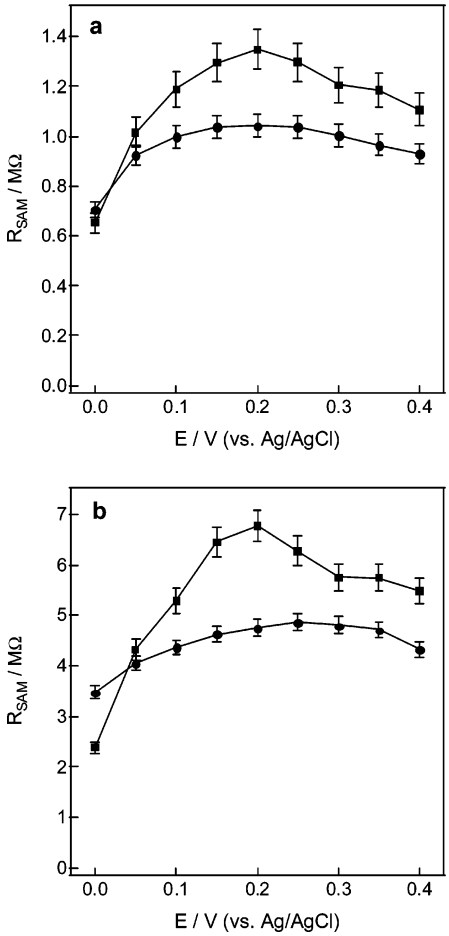

Figure 4. R_{SAM} for the shortTP monolayer as a function of the dc potential before (■) and after (●) addition of 100 μM aluminum ions. The electrolyte concentration and frequency range used for modeling were (a) 100 mM KNO_3 and 1000−10 Hz and (b) 10 mM KNO_3 and 100−2 Hz, respectively.

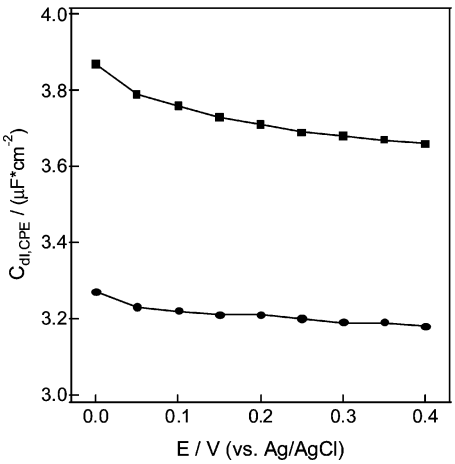

Figure 5. $C_{dl,CPE}$ for the shortTP monolayer as a function of the dc potential before (■) and after (●) addition of 100 μM aluminum ions. The electrolyte concentration and frequency range used for modeling were 100 mM KNO_3 and 1000−10 Hz, respectively.

indicating that R_{SAM} does not scale directly with the electrolyte concentration. This is probably related to several factors, for example, the influence from the ionic strength on the potential distribution at the interface.

From Figure 4, the influence from the dc potential on the number of ions in the monolayer was obvious. At more negative potentials, the presence of cations within the SAM is facilitated, and likewise for anions at more positive potentials.[29] The thiol organization on the surface may also change with the dc potential.[29−31] Although these two electric field effects are difficult to separate, their relative influence on R_{SAM}, compared to the influence from the aluminum ions, became more important at potentials close to 0.0 and 0.4 V. At potentials below 0.1 V in Figure 4a, the influence from the aluminum ions was, for example, no longer significant. An interesting observation from Figure 4a and b was also that the relative influence from the electrode potential was lower when aluminum ions were coordinated to the phosphate groups. This most likely reflects the fact that the phosphate charges then were neutralized and less able to change their organization on the surface. These first experiments show that the resistive properties of a functionalized SAM can be significantly changed upon a chemical interaction. The presence of ions within the SAM is also influenced by other factors, which may bring important information. As will be further discussed below, a maximum in R_{SAM} could, for example, also reveal the potential where the ionic conductivity within the monolayer is at minimum.[29]

The impedance measurements also gave information on the differential double layer capacitance. The total double layer capacitance for a SAM-covered electrode can basically be described by two capacitors in series, i.e., the capacitance of the SAM itself and the capacitance of the diffuse layer. The thickness and dielectric properties of the SAM are then together with the electrolyte conductivity the most important factors determining the interfacial capacitance. More complicated models have also been described in the literature. At the electrolyte concentrations used in this work, the total double layer capacitance is in practice dominated by the capacitance of the SAM; hence, only one component ($C_{dl,CPE}$) was used to represent the interfacial capacitance. In Figure 5, the total differential double layer capacitance for the shortTP monolayer is displayed as a function of the electrode potential in 100 mM KNO_3, both in the presence and in the absence of aluminum ions. As expected from previous results,[24,25] the capacitance dropped ~0.5 μF·cm^{-2} when aluminum ions were coordinated, as the charge or polarity of the phosphate groups then decreased. In general, the influence from the electrode potential was not large, although the capacitance was found to be slightly higher at the lowest values of R_{SAM}.[2] As discussed above, the capacitance was also more sensitive to changes in the electric field before addition of aluminum ions. The influence from the dc potential and aluminum ions were basically the same in 10 mM KNO_3 (data not shown), but the capacitances were then ~7−10% lower as a result of the decreased number of ions, both within the SAM itself and in the diffuse layer. The potential dependence of the capacitance in Figure 5 was slightly different compared to our previous work with phosphorylated serine and tyrosine analogue thiols. The present experiments may hence be a more advantageous way of evaluating the double layer capacitance, as changes in the capacitance to some extent simultaneously can be correlated to the resistive properties of the monolayer.

ShortTOH SAM. Exactly the same experiments were also performed with nonphosphorylated tyrosine thiols. These thiols lack the possibility to coordinate aluminum ions, and they are also uncharged. The structure of the resulting monolayer and the total double layer capacitance were hence previously not found to change when aluminum ions were added to the electrolyte.[25] In Figure 6, R_{SAM} for the shortTOH is displayed as a function of the electrode potential in (a) 100 and (b) 10 mM KNO_3, both before and after addition of aluminum ions. Although some data points were significantly different, there was in general no significant change in R_{SAM} when aluminum ions were added to the electrolyte. The absolute values of R_{SAM} were also found to be approximately the same as for the corresponding phosphorylated SAM in Figure 4. The influence from the electrode potential was on the other hand different. The hydroxyl-terminated tyrosine SAMs displayed a maximum in R_{SAM} around 0.10−0.15 V, and also a minimum around 0.30−0.35 V. Interestingly, the maximum in R_{SAM} for the shortTOH was situated at a more negative potential compared to the shortTP monolayer. This shift is probably related to the difference in charge and polarity of the functional group.[29]

The minimum in R_{SAM} coincided with a small minimum in the double layer capacitance, both in 100 and in 10 mM KNO_3 (see Figure 7 for the latter). The minimum was more pronounced in 10 mM KNO_3 and also before the aluminum ions were added to the electrolyte. A minimum in R_{SAM} could according to the discussion above indicate the potential where the ionic conductivity within the SAM is at maximum. This is, however, probably only a part of the explanation as there was also a dip in the capacitance in the same potential range. A minimum in the capacitance at lower supporting electrolyte concentrations indicates a minimum in the diffuse layer capacitance, which occurs at or near the potential of zero charge (pzc), i.e., the potential where there is no excess charge on the electrode surface. In the present experiments with shortTOH, 10 mM KNO_3 may hence be low enough so the diffuse layer capacitance significantly can influence the total interfacial capacitance (having in mind that the dip became smaller when aluminum ions were added to the

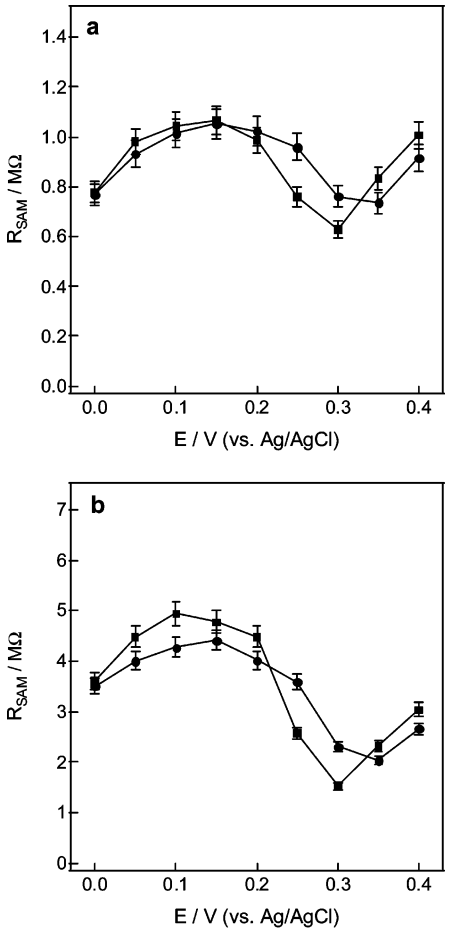

Figure 6. R_{SAM} for the shortTOH monolayer as a function of the dc potential before (■) and after (●) addition of 100 μM aluminum ions. The electrolyte concentration and frequency range used for modeling were (a) 100 mM KNO_3 and 1000−10 Hz and (b) 10 mM KNO_3 and 100−2 Hz, respectively.

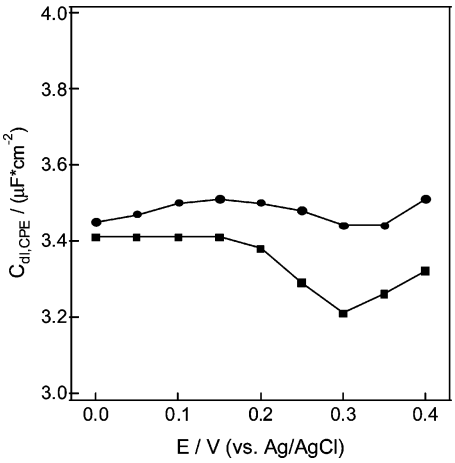

Figure 7. $C_{dl,CPE}$ for the shortTOH monolayer as a function of the dc potential before (■) and after (●) addition of 100 μM aluminum ions. The electrolyte concentration and frequency range used for modeling were 10 mM KNO_3 and 100−2 Hz, respectively.

solution). Although the exact relationship between R_{SAM} and the capacities of the SAM and the diffuse layer is at present not clear to us, the change to a nonphosphorylated functional group clearly gave different results. The understanding of the connection between the double layer capacitance and R_{SAM} would most likely benefit from a thorough study including a wide range of functionalized thiols, different solvents, and supporting electrolyte concentrations, and preferably also nonelectrochemical techniques (based on for example infrared spectroscopy and probe microscopy).

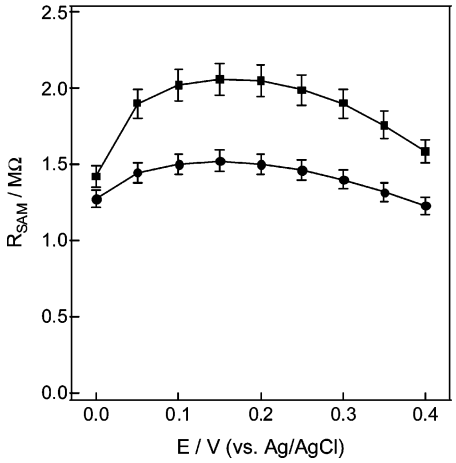

Figure 8. R_{SAM} for the longTP monolayer as a function of the dc potential before (■) and after (●) addition of 100 μM aluminum ions. The electrolyte concentration and frequency range used for modeling were 100 mM KNO_3 and 1000−30 Hz, respectively.

LongTP SAM. In order to also compare with a much better insulating SAM, the same experiments were performed with a phosphorylated tyrosine analogue having a longer carbon chain (Figure 1c). A longer carbon chain facilitates the organization on the surface and contributes to a more hydrophobic environment. A longer carbon chain also has the consequence that most of the potential drop at the interface will take place over the carbon chains. The variation of R_{SAM} for the longTP in 100 mM KNO_3 is presented in Figure 8. Compared to the shortTP in Figure 4a, R_{SAM} was now ~40−80% higher, a result from the thicker and better organized SAM, and of course also the more hydrophobic environment.[34] Approximately the same increase was also obtained in 10 mM KNO_3 (data not shown). The relative influence from the dc potential in Figure 8 was smaller compared to the shortTP in Figure 4, and the maximum in R_{SAM} was also shifted to a more negative potential. The addition of aluminum ions was also here found to have a significant influence on the thiol organization, in both 100 and 10 mM KNO_3. Considering the length of the extra carbon chain in the longTP SAM, it is somewhat unexpected that R_{SAM} only increased by 40−80%. This is most likely explained by the fact that the longTP thiols were assembled with protective *tert*-butyl groups on the phosphates. These groups are bulky, which may restrict the assembly on the surface and enable ions to penetrate into the monolayer, also after the deprotection. The $C_{dl,CPE}$ for the longTP was practically unchanged when aluminum ions were added and when the dc potential was changed. In 100 mM KNO_3, the capacitances were between 1.35 and 1.39 $\mu F \cdot cm^{-2}$ when the potential was varied between 0.0 and 0.4 V, and the same capacitances dropped to 1.28−1.33 $\mu F \cdot cm^{-2}$ when aluminum ions were added. The corresponding values in 10 mM KNO_3 were 1.23−1.27 and 1.19−1.21 $\mu F \cdot cm^{-2}$, respectively. The capacitance was hence dominated by the hydrophobic part of the SAM. For SAMs having good insulating properties, it could hence be a better alternative to evaluate a chemical interaction based on R_{SAM}, rather than the interfacial capacitance.

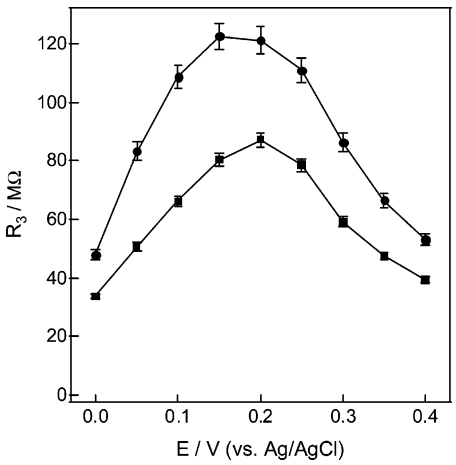

Figure 9. R_3 for the shortTP monolayer as a function of the dc potential before (■) and after (●) addition of 100 μM aluminum ions. The electrolyte concentration and frequency range used for modeling were 100 mM KNO_3 and 5−0.1 Hz, respectively.

The results shown for the three tyrosine SAMs demonstrate that EIS and relatively low excitation frequencies can be used to detect changes in the monolayer structure upon a chemical interaction at the ω-end. This type of experiments can hence provide useful information when using SAMs in model systems and as templates in, for example, sensor and detector applications. An important advantage is that it is not necessary to add a redox couple to the electrolyte. This is especially advantageous when surface modifications are to be studied at different dc potentials. Information on the ion permeation can also benefit the interpretation of the differential double layer capacitance, which is often used to evaluate chemical interactions or to investigate complex double layer phenomena. On the other hand, a drawback is that it is difficult to separate and quantify the different factors that influence the ion permeation. The variation of the electrode potential may also be used to indicate the potentials where the ionic conductivity within a SAM is at maximum or minimum. Based on results from methyl terminated alkanethiols with 15 methylene units, Protsailo and Fawcett[29] suggested a correlation between the maximum in R_{SAM} and the potential of zero charge. For one of the thiols in the present study, we rather experienced the opposite as the pzc coincided with a minimum in R_{SAM}. This indicates that the correlation between the ionic conductivity within a functionalized monolayer and the pzc is influenced by several factors. In the present case, there was, for example, most likely no clear boundary between the diffuse layer and the poorly insulating monolayer of more or less hydrophilic thiols.

ShortTP SAM at Frequencies between 1000 and 0.1 Hz. The impedance spectra for the shortTP were also found to contain further information at even lower frequencies. As shown in Figure 2b, a second semicircle is present between 5 and 0.1 Hz. The equivalent circuit in Figure 3a was first employed to evaluate this second *RC* process in the simplest possible way (the parallel resistance is now denoted as R_3 to separate it from R_{SAM}). The values of R_3 as a function of the dc potential are displayed in Figure 9. Similar to R_{SAM}, R_3 also has a maximum around 0.2 V, but the big difference is that the absolute values of R_3 are much higher. Another interesting difference was also that R_3 increased ~30% when aluminum ions were added to the solution.

Similar results for SAM-modified electrodes have previously been reported by others. For alkanethiol based SAMs, Boubour and Lennox[30,31] described an additional *RC* process related to potential-induced defects. They used an equivalent circuit with two *RC* elements for evaluation (see Figure 3b) and suggested that the extra *RC* circuit could be related to the monolayer's ability to store charge and the ease of moving an ion from the interface to the SAM. In a study including three different SAMs, Fawcett et al.[26] reported two *RC* processes for a SAM based on 4′-hydroxy-4-mercaptobiphenyl, but only when the supporting electrolyte concentration was 0.1 or 1 M. They used a slightly different equivalent circuit (Figure 3c) and suggested that the extra *RC* process could be due to different structural domains in the SAM. The interpretation of R_3 in the present experiments is at this point not clear. R_3 changes with the potential in a similar fashion as R_{SAM}, but the time constant for the former *RC* process is much larger. R_3 also increased after addition of aluminum ions, which indicates that R_3 may also be influenced by other factors than reorganization of the thiols on the surface. One suggestion is that R_3 is related to the polarity at the end of the monolayer, which drastically decreases when aluminum ions are added.[30] Our conclusion was also that the type of thiol and functional group, as well as the ionic strength, matters. It was, for example, not possible to evaluate R_3 when using the lower supporting electrolyte concentration, nor for the other two SAMs.

In an effort to simultaneously evaluate the two *RC* processes for the shortTP SAM, the equivalent circuits in Figure 3b and c were tested. When using the circuit in Figure 3b, R_3 was not significantly different from the results in Figure 9. The same was also true when using the circuit in Figure 3c; however, in this case R_3 was only increased by 20% after addition of aluminum ions. Although as many as 50 frequencies per decade were used, the simultaneous evaluation of the two processes were clearly influenced by each other. R_{sol} and $C_{dl,CPE}$ were the same when using the more advanced circuits, but their uncertainties became higher. The values of the second capacitance, $C_{2,CPE}$, were on the other hand difficult to interpret, and R_{SAM} also suffered from the more complex circuits. For both of them, the uncertainties were too large (20−80%) to make any valid interpretation. This was probably not related to an erroneous choice of circuits, but rather the fact that the absolute impedance ranges for the two processes were too different. For the present shortTP SAM, it was hence better to use a simpler equivalent circuit and evaluate each *RC* process separately. The results in this section, although difficult to interpret, indicate that very low frequencies can also be used to give additional information on chemical interactions at functionalized SAMs.

CONCLUSIONS

Electrochemical impedance spectroscopy and relatively low excitation frequencies were used to investigate ion permeation within ω-functionalized SAMs immobilized on gold electrodes. The ion permeation was evaluated by an extra resistive component in the equivalent circuit and was found to be influenced by structural changes in the monolayer and by electric fields. Although several questions still remain to be answered, it is clear that the presence of ions inside the monolayer is an important factor to consider when using SAMs. The present type of experiments may, for example, be a convenient way to find the potential where the ionic

conductivity within the SAM is at maximum or minimum, although the correlation to the potential of zero charge was not straightforward. The experiments may further benefit the evaluation of the interfacial capacitance, as the results at the same time can be related to the permeation of ions. An important advantage is that the experiments were made without any addition of redox species. The impedance spectra also revealed that frequencies below 5 Hz were useful under certain conditions, and those data may contribute to additional information on complex double layer phenomena. In a broader perspective, these kinds of experiments can be applied for analysis of many types of surface modifications where it is not advantageous to use faradaic currents. We are at present exploring the use of EIS and low frequencies for the analysis of other types of poorly insulating coatings, for example, thiolated polypeptides and hydrogels.

ACKNOWLEDGMENT

This project was supported by grants from The Carl Trygger Foundation, as well as from Vinnova and SSF (F.B.), and The Swedish Research Council (K.U.). Johan Ekeroth and Andreas Carlsson are acknowledged for synthesizing the tyrosine molecules.

Received for review July 2, 2007. Accepted August 17, 2007.

AC071399D